Available online at www.sciencedirect.com
ScienceDirect
Journal of Power Sources 173 (2007) 700–706
JOURNAL OF POWER SOURCES
www.elsevier.com/locate/jpowsour

Studies of selected synthesis procedures of the conducting $LiFePO_4$-based composite cathode materials for Li-ion batteries

W. Ojczyk [a], J. Marzec [a], K. Świerczek [a], W. Zając [a], M. Molenda [b], R. Dziembaj [b], J. Molenda [a,*]

[a] *Faculty of Materials Science and Ceramics, AGH University of Science and Technology, Al. Mickiewicza 30, 30-059 Kraków, Poland*
[b] *Faculty of Chemistry, Jagiellonian University, ul. R. Ingardena 3, 30-060 Kraków, Poland*

Available online 21 May 2007

Abstract

In this paper technological aspects of a synthesis of phospho-olivine $LiFePO_4$ based composite cathode materials for lithium batteries are presented. An effective synthesis route yielding a highly conductive composite cathode material was developed. The structural, electrical and electrochemical properties of these materials were investigated. It was shown that the enhanced conductivity of the cathode material is due to the presence of a thin layer of the reduced material which has metallic properties, which is formed on the grain surfaces of the phospho-olivine. We propose a synthesis route yielding $LiFePO_4/Fe_2P$ composite material.
© 2007 Elsevier B.V. All rights reserved.

Keywords: Lithium battery; $LiFePO_4$; Olivines; Iron phosphides or carbophosphides

1. Introduction

The $LiMXO_4$ type compounds (M = metal 3d, X = S, P, As, Mo, W) represent a novel group of electrode materials for reversible lithium ion cells [1]. In this group, $LiFePO_4$ with an olivine structure is the most promising one. This material exhibits several outstanding features, such as a high gravimetric capacity (170 mAh g^{-1}), thermal stability, high voltage towards lithium (~3.5 V) and low cost production. However, the application of $LiFePO_4$ in Li-ion batteries technology is hindered, because of the extremely low electric conductivity, of the order of 10^{-10} S cm^{-1}, at room temperature. Recently, encouraging reports were published, concerning spectacular enhancements of the electric conductivity in the case of doped olivine $LiFePO_4$ [2]. It was reported [2] that the conductivity can be increased by a factor of 10^7 by doping the lithium sublattice in $LiFePO_4$ with Nb^{5+}, Zr^{4+}, Mg^{2+} ions. Soon after, a theoretical work based on ab initio methods was published [3], providing evidence for possible metallic properties of the olivines, which resulted from the doping process. Nevertheless, the investigations subsequently carried out over the surface of the doped olivine have shown that the high values of the electric conductivity obtained are related to the formation of metallic iron phosphides or carbophosphides, located on the surface of the $LiFePO_4$ phase grains [4,5]. These experiments clearly demonstrated that the macroscopic metallic properties observed were not associated with the bulk properties of the material. The formation of iron phosphides or carbophosphides on the $LiFePO_4$ surface is caused by reducing factors at the initial stages of the synthesis process.

In this work, we present the technology of preparation of the conducting composite $Fe_2P/LiFePO_4$.

2. Experimental

Phospho-olivine $LiFePO_4$ was obtained by the high temperature synthesis route. The following compounds were used as starting materials: Li_2CO_3 (POCH—Gliwice, spectral purity), $FeC_2O_4 \cdot 2H_2O$ (Sigma Aldrich, 99%), $NH_4H_2PO_4$ (POCH—Gliwice, analytical grade). The starting materials were weighed on an analytical balance having an accuracy of 0.1 mg. For better homogeneity of the mixture, the starting materials were milled using a rotating-vibrating mill. Commercially available zirconia milling balls, 5 mm in diameter, were used for milling. In order to achieve the best efficiency of milling a ball/powder weight ratio of 1:20 with the chamber filling ratio

* Corresponding author. Tel.: +48 12 6172522; fax: +48 12 6172522.
E-mail addresses: molenda@agh.edu.pl, molenda@uci.agh.edu.pl (J. Molenda).

0378-7753/$ – see front matter © 2007 Elsevier B.V. All rights reserved.
doi:10.1016/j.jpowsour.2007.05.055

Table 1
Stages of the phospho-olivine $LiFePO_4$ synthesis

Stage	Temperature (°C)	Annealing time (h)
(a)	100	1.5
(b)	350	3.5
(c)	750	12

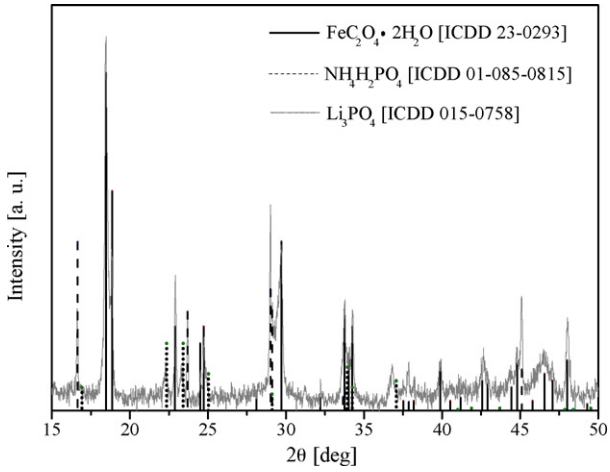

Fig. 1. A diffraction pattern for the substrates after milling in a rotating–vibrating mill.

of 3/4 was used. The working fluid was acetone of analytical grade. The milling process was carried out in 2 h.

The procedure developed for obtaining a pure $LiFePO_4$ involves several stages. To improve the argon purity a purifying system was employed for steam and oxygen removal. The particular stages and the annealing periods are listed in Table 1.

The main objective of the studies of the synthesis route for phospho-olivines was to determine the conditions facilitating the formation of an iron phosphide Fe_2P phase on the surface of $LiFePO_4$ grains. According to the literature [4], a slight lithium deficiency during the synthesis promotes the formation of the phosphides as a second phase. Therefore, for synthesis Li_xFePO_4 samples with nominal lithium content $x = 0.99$ and 0.97 were chosen. In order to optimize conditions favourable for the formation of the phosphide phase, four different approaches were employed (series I, II, III and IV, Table 2), with different heating rates for the starting materials and the argon flow through the flow reactor. Prior to synthesis, the entire system was flushed with a high purity argon (99.999% and $O_2 < 0.0005\%$). After the

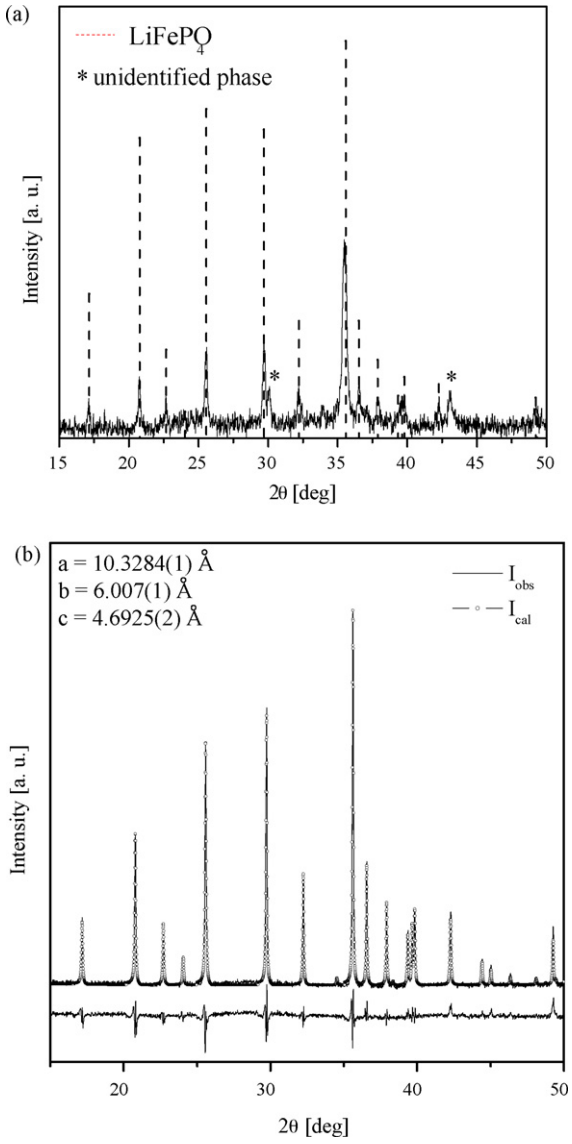

Fig. 2. A diffraction pattern for the substrates after annealing at 350 °C (a) and at 750 °C (b)—a synthesis procedure according to Table 1.

annealing at 600 °C the materials were slowly cooled down to room temperature. Next, the samples were ground in a mortar and then uniaxially pressed at 500 MPa. The pellets obtained were again placed in a furnace. Again, at the beginning of every stage the synthesis system was re-purified. The subsequent stage was carried out at 800 °C (Table 2).

Table 2
Different approaches towards synthesis route within the temperature range of 350–800 °C

Series I—flow: 20 cm^3 min^{-1} Ar	Series II—flow: 20 cm^3 min^{-1} Ar	Series III—flow: 200 cm^3 min^{-1} Ar	Series IV—flow: 200 cm^3 min^{-1} Ar
350–600 °C			
40 min to reach 350 °C	5 h to reach 350 °C	40 min to reach 350 °C	5 h to reach 350 °C
8 h annealing in 350 °C	8 h annealing in 350 °C	8 h annealing in 350 °C	8 h annealing in 350 °C
40 min to reach 600 °C	5 h to reach 600 °C	40 min to reach 600 °C	5 h to reach 600 °C
8 h annealing in 600 °C	8 h annealing in 600 °C	8 h annealing in 600 °C	8 h annealing in 600 °C
600–800 °C			
2 h to reach 800 °C	7 h to reach 800 °C	2 h to reach 800 °C	7 h to reach 800 °C
8 h annealing in 800 °C	8 h annealing in 800 °C	8 h annealing in 800 °C	8 h annealing in 800 °C

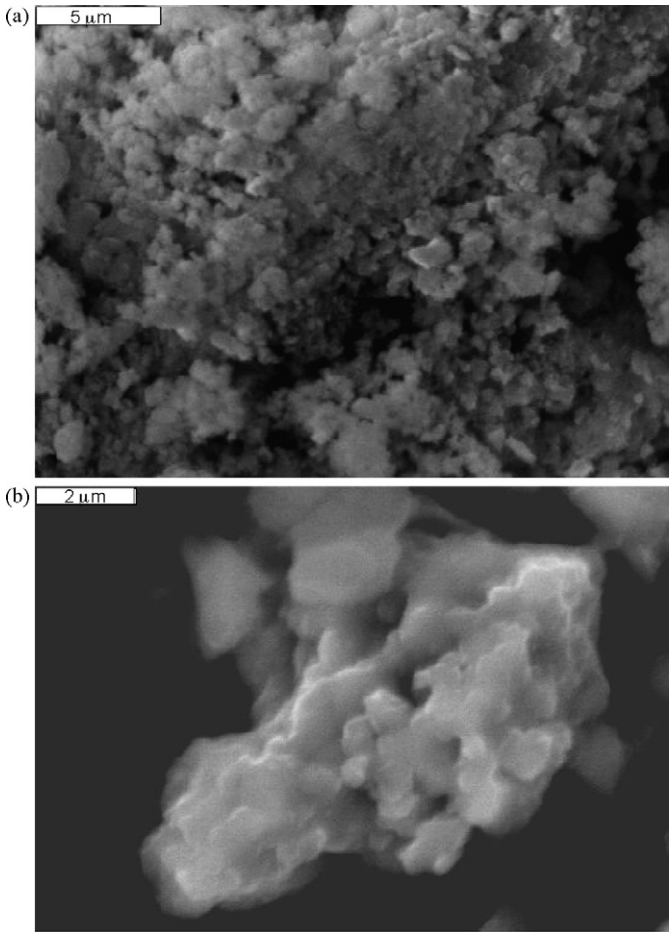

Fig. 3. SEM images of the material after annealing in 350 °C (a) and 750 °C (b)—a synthesis procedure according to Table 1.

After annealing at 800 °C the samples were cooled in the furnace under a steady argon flow down to room temperature.

The morphology of the materials obtained was characterized by means of scanning electron microscopy (SEM). The EDS investigations performed allowed for an analysis of the spatial distribution of chemical elements in the samples. The results of

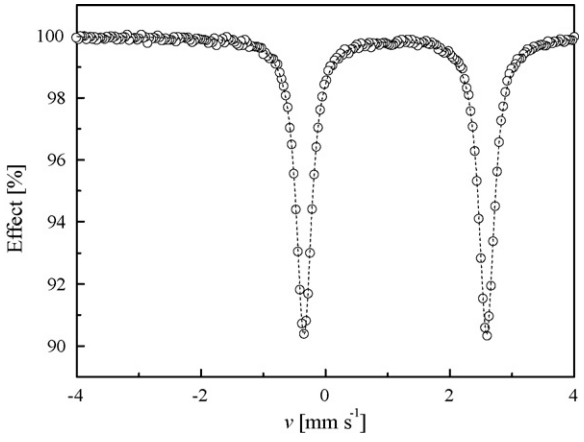

Fig. 4. Moessbauer spectrum for $LiFePO_4$ obtained according to the synthesis procedure from Table 1.

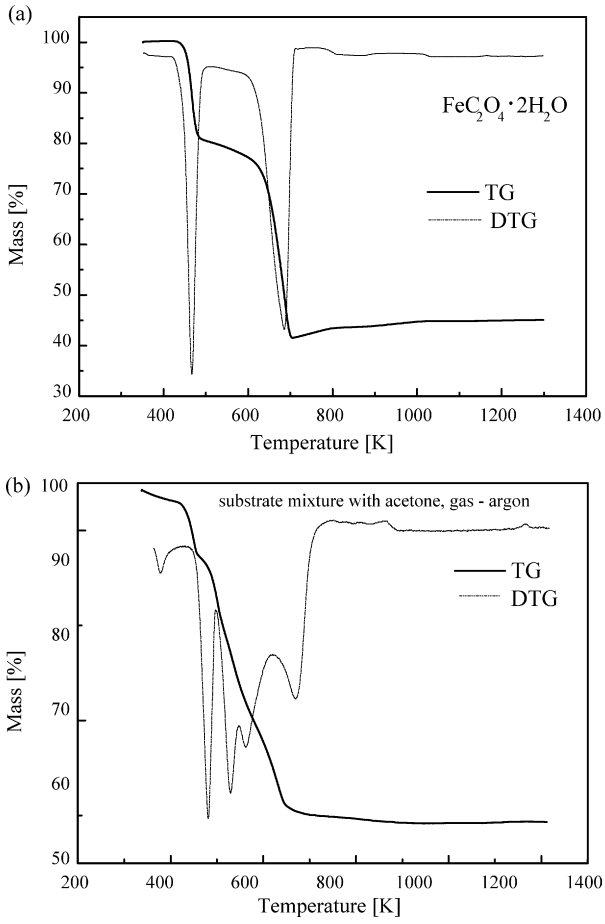

Fig. 5. A TG curve of iron oxalate dihydrate (a) and the initial mixture of the substrates (b).

XRD together with the Rietveld analysis helped to determine the phase composition of the materials.

TEM (transmission electron microscopy) observations were carried in order to reveal the presence of iron- and phosphorus-enriched and oxygen-depleted areas thus confirming the electron conducting phosphide or carbophosphide phases, located at

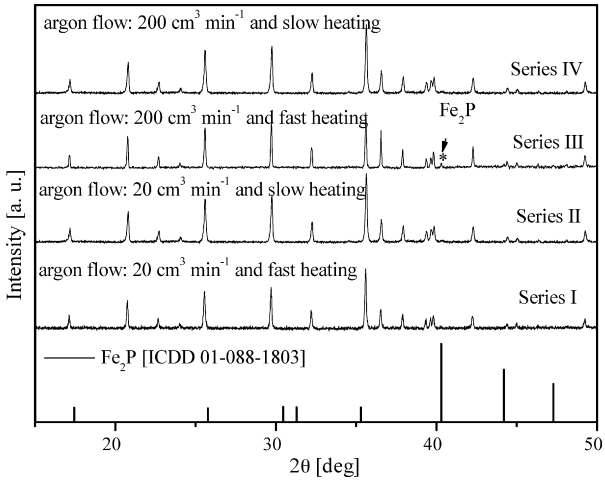

Fig. 6. A comparison between the diffraction patterns obtained for the samples prepared by different synthesis routes (series I, II, III and IV), following the description given in Table 2.

the grain boundaries. Thermogravimetric measurements of the initial mixtures and iron oxalate were conducted using a Mettler-Toledo 851^e apparatus in a dry argon flow (80 $cm^3\,min^{-1}$), over a temperature range of 350–1300 K and a heating rate of 5 $K\,min^{-1}$. Electrical conductivity measurements were performed by means of the dc four-probe method in the temperature range 125–500 K. Thermoelectric power was measured using a dynamic method with a variable temperature gradient in the temperature range 150–320 K. Electrochemical characterization of the cathode materials was carried out in electrochemical cells with a metallic lithium anode. The electrolyte used was a 1 M solution of $LiClO_4$ in 1:1 ethylene carbonate/dimethyl carbonate (EC/DEC).

3. Results and discussion

3.1. Preparation of a pure $LiFePO_4$ phase

Fig. 1 presents the diffraction pattern of a Li_2CO_3, $FeC_2O_4{\cdot}2H_2O$ and $NH_4H_2PO_4$ mixture after milling in a vibrating–rotating mill. Phase analysis revealed the presence of lithium phosphate, indicating a chemical reaction between substrates $NH_4H_2PO_4$ and Li_2CO_3, which results in Li_3PO_4 formations. The reaction can be described as follows:

$$2NH_4H_2PO_4 + 3Li_2CO_3 \rightarrow 2Li_3PO_4 + 2NH_{3\,aq} + 3CO_2\uparrow + 3H_2O \quad (1)$$

The diffraction patterns and SEM images of the mixture after annealing in 350 and 750 °C (the synthesis route according to Table 1) are shown in Figs. 2a and b and 3a and b, respectively. The results presented in Fig. 2a indicate that the olivine phase is formed already at 350 °C. Small amounts of impurities are also present. SEM images show small crystallites appearing at 350 °C, which is also confirmed by the results of the XRD analysis. The size of the crystallites was estimated to be about 100–200 nm from the XRD reflections half-width. The results for the material after the annealing at 750 °C demonstrate that a pure, monophase sample of olivine structure *Pnma* was obtained. The SEM image (Fig. 3b) implies the crystallites

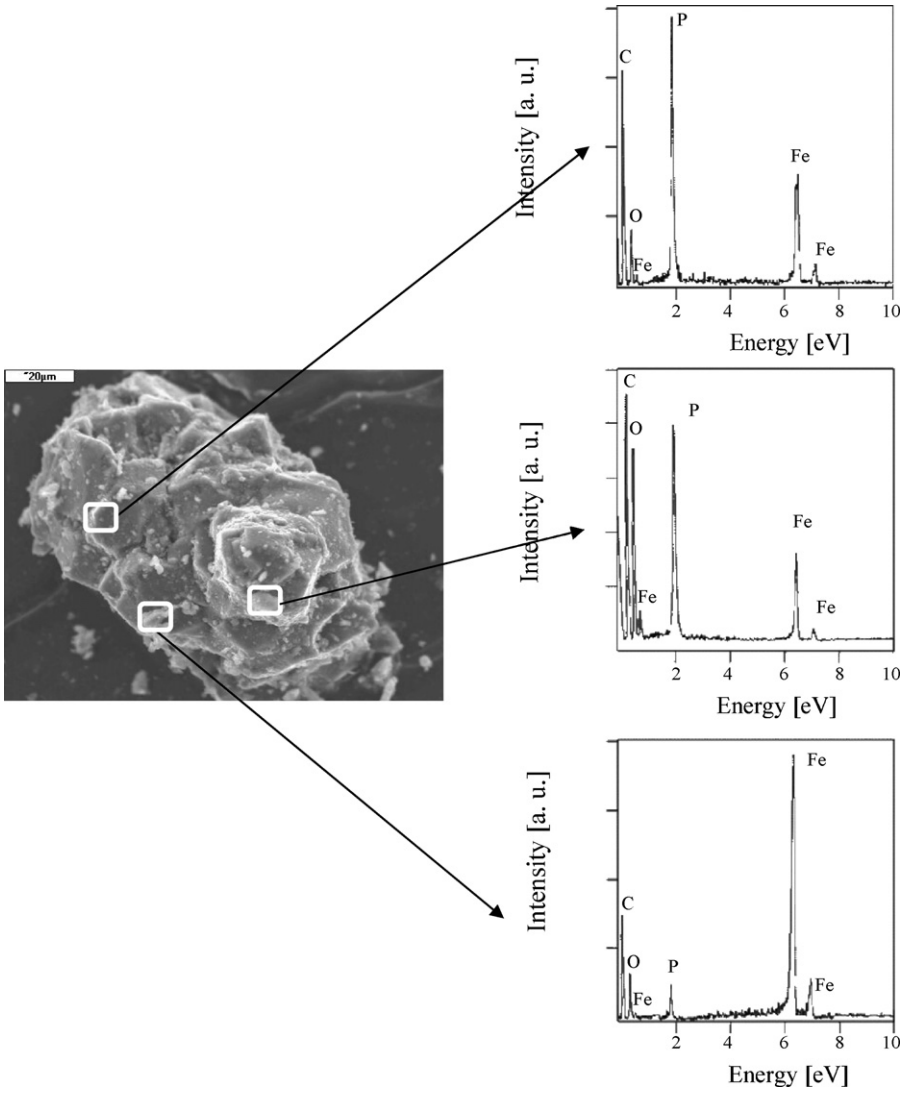

Fig. 7. SEM and EDS results for the sample obtained according to the procedure for series III (Table 2).

aggregation at this stage of the synthesis. Mossbauer spectroscopy measurements were performed (Fig. 4) and the results indicate only one quadruple doublet with an isomeric shift equal to IS = 1.2 mm s^{-1}, which is characteristic for Fe^{2+}.

3.2. Preparation of a composite phase $LiFePO_4$–Fe_2P

The presence of a highly reducing agent is necessary for a successful preparation of the Fe_2P phase. Such a reducing agent should be formed during the synthesis process, being an intermediate product of the reaction. The analysis of chemical properties of the particular substrates indicates that the reducing agent is probably formed as the product of the $FeC_2O_4{\cdot}2H_2O$ thermal decomposition reaction. However, the results of the thermal analysis (MS-TGA/DTG) results carried out over the thermal decomposition of $FeC_2O_4{\cdot}2H_2O$ has shown that the mechanism of the decomposition reaction strongly depends on the reaction environment. Our investigations demonstrated that the maximum amount of the reducing agent, namely fine dispersed iron nanoparticles, was obtained during the decomposition carried in a dry argon flow. This condition seems to be crucial, since the presence of steam in the reaction environment causes a secondary oxidation of iron and a consequently disappearance of the reducing agent, according to the reaction:

$$3Fe + 4H_2O \rightarrow Fe_3O_4 + 4H_2\uparrow \quad (2)$$

A formation of the lower oxides is also possible in the case of the steam deficiency (the oxidizing agent). A uniform dispersion of the reducing agent is also required for the creation of the Fe_2P thin layer on the $LiFePO_4$ phospho-olivine surface. On the basis of the synthesis tests previously performed we found that the best results were achieved for the reaction mixtures milled in a ball mill.

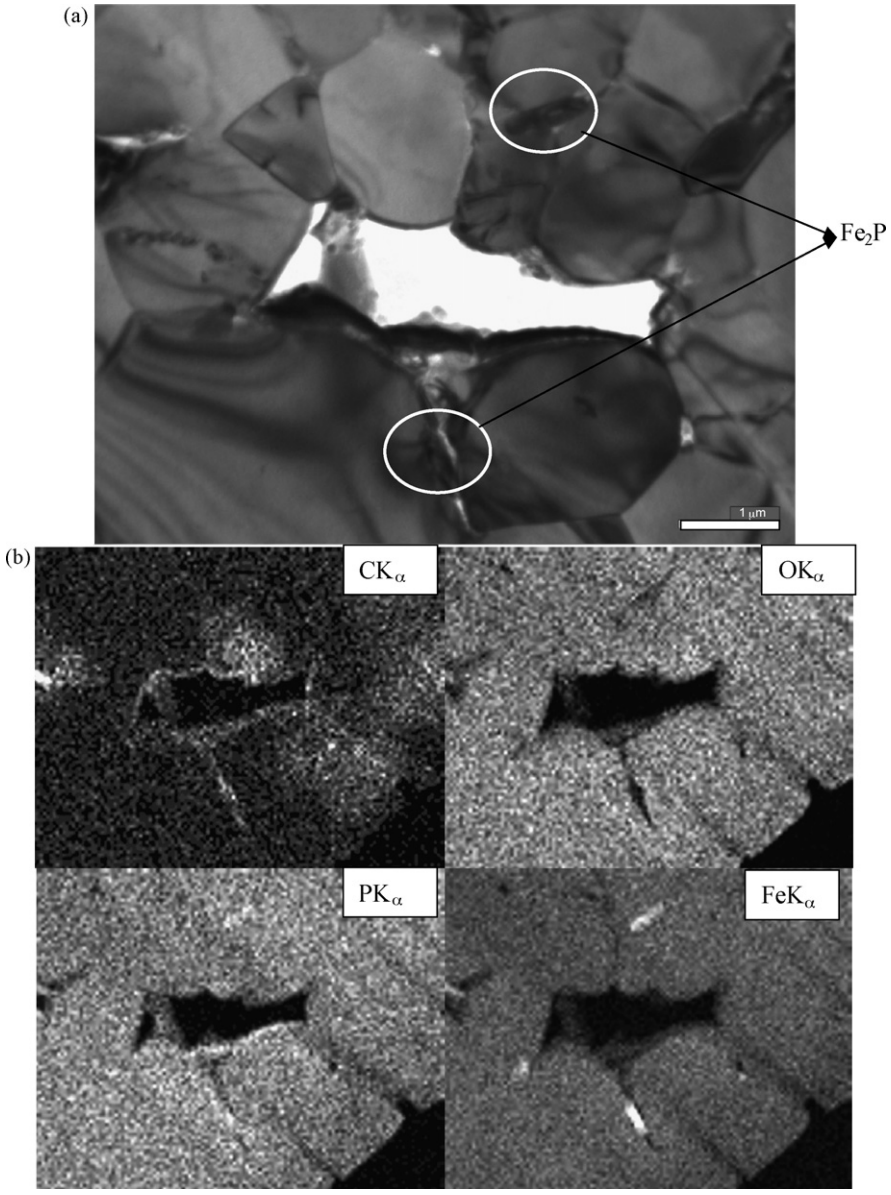

Fig. 8. A TEM image (a) and map of elements distribution for sample obtained by means of procedure III (Table 2) (b).

Iron nanoparticles as the reducing agent are highly unstable in the presence of trace amounts of oxygen. Still, when they are rapidly exposed to the environment with a high concentration of oxygen (such as air), the nanoparticles may undergo a passivation reaction (surface oxidation and the formation of a protective, gas-tight oxide layer). In our case, it can be assumed that the oxide layer, resulting from the passivation prevented the oxidation of the reducing agent with oxygen from air at the intermediate stage of the synthesis, i.e. milling of the mixture after the calcination in 350 °C.

The formation of iron phosphide Fe_2P resulting from the reduction of phosphate radicals with iron nanoparticles occurs only at higher temperatures (above 600 °C). Below this temperature iron can be oxidized with oxygen residues. Consequently, the exposure time of the reaction mixture at low temperatures should be as short as possible. Therefore, high rates of the furnace heating up to the optimum reaction temperature are essential. The results of a thermal analysis for the reaction mixtures yielded a temperature of 800 °C for 10 h at the optimum synthesis conditions.

Fig. 5a presents the thermal decomposition of an iron oxalate dihydrate whereas Fig. 5b shows the mass losses for the initial reaction mixture annealed under a dry argon atmosphere. XRD patterns for the samples are shown in Fig. 6. It can be seen that the phosphide phase Fe_2P appears in the materials obtained according to the procedure for series III, i.e. a massive argon flow and fast heating (Table 2).

Fig. 7 shows SEM image for the material prepared according to the procedure for series III (see Table 2). EDS analysis showed a rather uneven distribution of elements, despite the fact that the dominating phase of this sample is $LiFePO_4$ (see Fig. 6). The presence of iron and phosphorus-enriched with simultaneously oxygen depleted areas is observed. Therefore, it can be concluded that iron phosphides occur in the form of small inclusions. For exclusively iron-enriched areas, a possible explanation is the presence of nanoparticle iron residues, being a product of iron oxalate dihydrate thermal decomposition.

Fig. 8a presents the TEM image of the composite material for a polished section. EDS analysis (Fig. 8b) confirmed the presence of phosphorus, iron and carbon-enriched areas in the sample. The iron and phosphorus-enriched areas appear in the form of small inclusions, and the distance between them is about 3 μm. At the same time, the areas rich in carbon are located at the grain boundaries. It seems likely that contact between the phosphide inclusions is provided by carbon.

Thermal dependencies of electrical conductivity and thermoelectric power for the phospho-olivine samples $Li_{0.99}FePO_4$ and $Li_{0.97}FePO_4$ are shown in Fig. 9a and b, respectively. The samples were obtained according to the procedure for series III, i.e. they contained metallic inclusions of Fe_2P. The estimated activation energy of the electrical conductivity for both samples is practically the same and is equal to 0.045 eV. This is related to the charge transport across the metallic inclusions of the phosphides. The observed increase in the conductivity of $Li_{0.97}FePO_4$ sample can be accounted for by the increased number of phosphide inclusions. Low values of the thermoelectric power of the order of few $\mu V\,K^{-1}$, together with the character of temperature

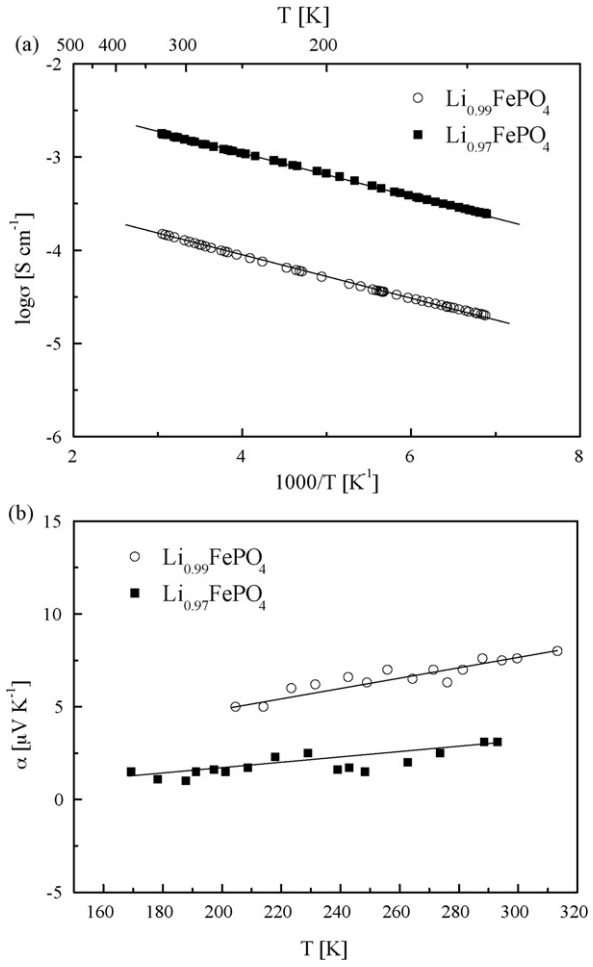

Fig. 9. Electrical conductivity (a) and thermoelectric power (b) dependence as a function of temperature for $Li_{0.99}FePO_4$ and $Li_{0.97}FePO_4$ samples (series III).

dependence indicate metallic type conductivity across the Fe_2P inclusions.

Fig. 10 presents charging curves of $Li/Li^+/Li_xFePO_4$ cells for chosen current densities. It can be seen that for high charging currents (*C*/5) the material utilizes only 20% of a theoretical

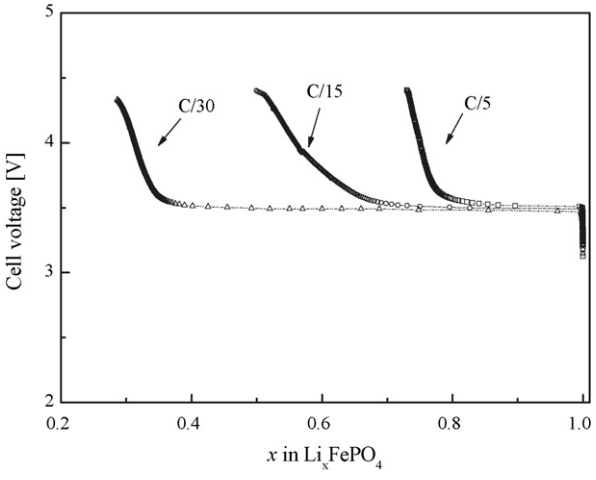

Fig. 10. Charge curves of $Li/Li^+/Li_xFePO_4$ cells. The starting material was $Li_{0.97}FePO_4$.

capacity. For small charging currents ($C/30$) more than 70% of the theoretical capacity can be achieved.

4. Conclusions

Taking into considerations the results of the thermal analysis and the synthesis trials, we propose the following conditions for the $LiFePO_4/Fe_2P$ composite synthesis process:

- Preparation of the Fe_2P phase requires the presence of a reducing agent—fine dispersed iron nanoparticles, being the intermediate product of $FeC_2O_4{\cdot}2H_2O$ thermal decomposition.
- The reducing agent is unstable and oxidizes easily by the oxygen residues, or steam resulting from decomposition reaction.
- A thin layer of Fe_2P can be formed provided that the reducing agent is highly dispersed, hence the necessity of milling the reaction mixture in a ball mill.

On the basis of the obtained results of thermal analysis and synthetic route trials it can be concluded that the requirements mentioned below can be met only when the appropriate conditions of the synthesis process are satisfied:

- The products of the reaction (H_2O) can be carried away properly from the reactor at the volume flow rate (F_v) of the carrying gas (Ar = 99.999%, $O_2 < 0.0005\%$) being at least:

$$F_v = 20 V_{\text{react}} t \text{ for 1 g of the reagents batch}$$

where F_v is the volume flow rate ($cm^3\ min^{-1}$) V_{react} the pipe flow reactor volume (cm^3), t the time = 60 min, both at the initial stage of the decomposition (350 °C) and the main high-temperature reaction (800 °C):

- Linear rate of carrying gas over the reagents w should be at least $0.5\ cm\ s^{-1}$; this would prevent secondary reactions (iron oxidation).
- Milling the substrates in a ball mill prior to the reaction ensures an appropriate dispersion of the substrates.
- A high heating rate ($\beta = 10\ K\ min^{-1}$), ensuring the maximum concentration of the reductive agent at the optimal temperature of the reaction (800 °C).

Acknowledgements

This work has been financially supported by the Polish Ministry of Science and Higher Education. The authors gratefully acknowledge prof. dr hab. inż. P. Zięba and dr hab. inż. J. Morgiel for providing help in carrying out TEM observations.

References

[1] K. Padhi, K.S. Nanjundaswamy, J.B. Goodenough, J. Electrochem. Soc. 144 (4) (1997) 1188.
[2] S.-Y. Chung, J.T. Bloking, Y.-M. Chiang, Nat. Mater. 1 (2002) 123.
[3] C. Lampe-Onnerud, S. Dalton, P. Onnerud, D. Novikov, J. Shi, J. Treger, R. Chamberlain, Proceedings of the 203rd Meeting of the Electrochemical Society, April 27–May 2, 2003.
[4] P.S. Herle, B. Ellis, N. Coombs, L.F. Nazar, Nat. Mater. 3 (2004) 147.
[5] J. Marzec, W. Ojczyk, J. Molenda, Mater. Sci. Poland 24 (2006) 69.